 CMES, vol.102, no.4, pp.257-270, 2014

Direct Volume-to-Surface Integral Transformation for 2D BEM Analysis of Anisotropic Thermoelasticity

Y.C. Shiah[1], **Chung-Lei Hsu**[1] **and Chyanbin Hwu**[1,2]

Abstract: As has been well documented for the boundary element method (BEM), a volume integral is present in the integral equation for thermoelastic analysis. Any attempt to directly integrate the integral shall inevitably involve internal discretization that will destroy the BEM's distinctive notion as a true boundary solution technique. Among the schemes to overcome this difficulty, the exact transformation approach is the most elegant since neither further approximation nor internal treatments are involved. Such transformation for 2D anisotropic thermoelasticity has been achieved by Shiah and Tan (1999) with the aid of domain mapping. This paper revisits this problem and presents a modified transformation for 2D anisotropic thermoelasticity, where no domain distortion is involved. Being defined in the original Cartesian coordinate system, the volume integral is analytically transformed to the boundary using the Stroh formalism. This transformation is favorable especially when the corresponding anisotropic field is directly calculated without resorting to the domain mapping technique. In the end, numerical examples are provided to show the validity of such a transformation.

Keywords: Direct volume-to-surface integral transformation, 2D anisotropic thermoelasticity, boundary element method.

1 Introduction

In engineering practice, thermoelastic analysis often plays an important role to ensure the integrity of structures when subjected to thermal loads. Being recognized as an efficient numerical tool, the BEM is characterized by its notion that only the boundary needs to be modeled. However, for treating thermal effects, an additional volume integral appears in the boundary integral equation (BIE) that shall destroy the BEM's notion as a truly boundary solution technique. This is because any means to directly integrate the extra volume integral will inevitably in-

[1] Dept. of Aeronautics and Astronautics, National Cheng Kung University, Taiwan, R.O.C.
[2] Correspondence. E-mail:ycshiah@mail.ncku.edu.tw, Tel:+886-6-757575 ext.63623

volve "cell" discretization throughout the whole domain. Over the years, there have been several techniques proposed to avoid such domain discretization, such as the Monte Carlo method [Gipson and Camp (1985)], the particular integral approach [Lachat (1975); Deb and Banerjee (1990)], the dual reciprocity method [Nardini and Brebbia (1982)], the multiple reciprocity method [Nowak and Brebbia (1989)], and the exact transformation method [Rizzo and Shippy (1977)], abbreviated as ETM herein. Among these schemes mentioned above, the ETM is fundamentally the most appealing because it restores the BEM analysis as a purely boundary solution technique yet without involving further numerical approximation and internal treatments per se. Although the ETM had been widely employed to treat equivalent body-force effects in isotropic elasticity, such a transformation for 2D anisotropic elasticity was not achieved until Zhang *et al.* (1997) first derived the transformed boundary integrals for 2D elastic analysis involving body forces. Following this success, Shiah and Tan (1999) proposed a volume-to-surface integral transformation by use of domain mapping, through which the thermal field is mapped onto an equivalent "isotropic" domain. Accounting for anisotropic effects, this coordinate transformation enables the use of Green's 2nd Identity to exactly transform the volume integral into boundary ones (Shiah and Tan, 1999), albeit defined in the new coordinate system. Following this success, Shiah *et al.* (2005) extended such treatment to the thermoelasticity problem when concentrated heat sources were present. Also, this scheme has been applied by Shiah and Tan (2000) to the problem of thermoelastic fracture of dissimilarly joined anisotropic materials. Applying this approach, Shiah et al. (2010) further derived the Somigliana Identity for the thermoelastic analysis at interior points. Such an approach for treating 3D thermoelastic analysis in generally anisotropic bodies has remained extremely scarce, if there is any. The only one that can be found to our best knowledge is presented by Shiah and Tan (2012), which simply treats transversely isotropic bodies. All kernel functions used in the references listed above for the 2D problems are based upon the formulations given by Lekhnitskii (1981). Generally speaking, this transformation works well as a subsequent elastic analysis after solving the thermal field by the domain mapping technique. However, when the anisotropic thermal field is to be solved directly, such a treatment appears to be less straightforward.

In this paper, a modified transformation process is presented to directly treat the 2D anisotropic thermoelasticity, where no coordinate transformation is involved. All fundamental solutions in the derivations are based upon the Stroh formalism [Hwu (2010)]. For demonstrating the validity of the transformation and of our implementation in the BEM analysis, a few numerical examples are presented in the end.

2 BIE for 2D anisotropic thermoelasticity

For generally anisotropic elastic media in two dimensions, the constitutive law between stresses σ_{ij} and strains ε_{ij} with thermal effects is governed by the well-known Duhamel-Neumann relation, that is

$$\sigma_{ij} = C_{ijkl}\varepsilon_{kl} - \beta_{ij}\Theta \quad , \tag{1}$$

where Θ is the temperature change, C_{ijkl} are the material stiffness coefficients, and β_{ij} represents the thermal moduli, given by $\beta_{ij} = C_{ijkj}\alpha_{kl}$, α_{kl} being the coefficients of linear thermal expansion. The effective values of stiffness and thermal moduli depend on the corresponding condition of either planestress or plane-strain For the steady-state condition without heat source, the anisotropic temperature field is governed by

$$k_{ij}\Theta_{,ij} = 0, \tag{2}$$

where k_{ij} denotes the heat conductivity coefficients By the sequentially coupled manner, the temperature field is first calculated for all thermal data on boundary nodes, followed by the subsequent elastic analysis. Since this thermal analysis is not the focus, it will not be further discussed here. So, all the following processes just take the thermal data as known values, determined via the usual BEM analysis as stated.

For a linear elastic body with thermal effects in the domain Ω, the displacement u_j and traction t_j on the boundary surface Γ are cross-related with each other by the well known BIE as follows:

$$\begin{aligned} &c_{ij}(\xi)u_j(\xi) + \int_\Gamma T^*_{ij}(\xi,\mathbf{x})u_j(\mathbf{x})d\Gamma(\mathbf{x}) \\ &= \int_\Gamma U^*_{ij}(\xi,\mathbf{x})t_j(\mathbf{x})\, d\Gamma(\mathbf{x}) + \int_\Omega \Theta(\mathbf{x})\beta_{jk}U^*_{ij,k}(\xi,\mathbf{x})\, d\Omega(\mathbf{x}) \end{aligned} \quad , \tag{3}$$

where $c_{ij}(\xi)$ are the geometric coefficients of the source point ξ; $U^*_{ij}(\xi,\mathbf{x})$ and $T^*_{ij}(\xi,\mathbf{x})$ are the fundamental solutions of displacements and tractions. As the main issue of the present work, the last integral in Eq.(3) is a volume integral that needs to be transformed to the boundary. In this study, the fundamental solutions are based on the complex-variable Stroh formalism for anisotropic elasticity, which can be written in a matrix form as [Hwu (2010)]

$$[U^*_{ij}] = \mathbf{U}^* = 2Re\{[\mathbf{AF}(z)]^T\}, \tag{4a}$$

$$[T^*_{ij}] = \mathbf{T}^* = 2Re\{[\mathbf{BF}_{,s}(z)]^T\}, \tag{4b}$$

where

$$\mathbf{F}(z_\alpha) = \frac{1}{2\pi i} < \ln(z_\alpha - \hat{z}_\alpha) > \mathbf{A}^T. \tag{5}$$

In Eq.(4a) and (4b), $\mathbf{A}$ and $\mathbf{B}$ are the material eigenvector matrices, Re{} denotes taking the real part of a complex value, the superscript T represents the transpose of a matrix, and $\mathbf{F}_{,s} = \partial\mathbf{F}/\partial s$gives the derivative of $\mathbf{F}$ along s, the tangential path of the body. The angular bracket in Eq.(5) stands for a 3×3 diagonal matrix, in which each element varies with the index α. In the above equations, the general complex variables z_α and $\hat{z}_\alpha$ for the field point and the source point, located respectively at $\mathbf{x} = (x_1, x_2)$ and $\xi = (\hat{x}_1, \hat{x}_2)$, are defined by

$$z_\alpha = x_1 + \mu_\alpha x_2, \quad \hat{z}_\alpha = \hat{x}_1 + \mu_\alpha \hat{x}_2, \tag{6}$$

in which μ_α (α=1,2) are the material's eigenvalues.

In the sequentially coupled manner, the temperature data, determined independently via solving the BIE for the associated field problem, are treated as the known values in Eq.(3). The work aims at transforming the volume integral into surface ones. For brevity, the volume integral is denoted by

$$V_i = \int_\Omega \Theta(\mathbf{x}) \beta_{jk} U^*_{ij,k}(\xi, \mathbf{x})\, d\Omega(\mathbf{x}). \tag{7}$$

Consider the following identity:

$$\int_\Omega (f_i k_{jk} \Theta_{,jk} - \Theta k_{jk} f_{i,jk})\, d\Omega = \int_\Omega [(f_i k_{jk} \Theta_{,j})_{,k} - (\Theta k_{jk} f_{i,k})_{,j}]\, d\Omega, \tag{8}$$

where f_i is the component of an arbitrary function f. As a result of applying the Green's 2nd Identity to the right hand side of Eq. (8), one immediately obtains

$$\int_\Omega (f_i k_{jk} \Theta_{,jk} - \Theta k_{jk} f_{i,jk})\, d\Omega = \int_\Gamma (f_i k_{jk} \Theta_{,j} n_k - \Theta k_{jk} f_{i,k} n_j)\, d\Gamma \tag{9}$$

From the relation in Eq. (2), the first term in the integrand on the left hand side of Eq. (9) vanishes and thus, Eq. (9) becomes

$$\int_\Omega \Theta k_{jk} f_{i,jk} d\Omega = -\int_\Gamma (f_i k_{jk} \Theta_{,j} n_k - \Theta k_{jk} f_{i,k} n_j) d\Gamma. \tag{10}$$

It immediately follows that by making the following substitution

$$k_{jk} f_{i,jk} = \beta_{jk} U^*_{ij,k}, \tag{11}$$

one obtains

$$V_i = \int_\Gamma (\Theta k_{jk} f_{i,k} n_j - f_i k_{jk} \Theta_{,j} n_k)\, d\Gamma. \tag{12}$$

Now, the task remains to determine the explicit expression of f_i according to Eq. (11). Let $f$be denoted by $f(z_\alpha)$ in what follows for the derivations. Expansion of Eq. (11) results in the following matrix form:

$$k_\alpha f_i'' (z_\alpha) = \boldsymbol{\beta}_1^T \mathbf{u}_{i,1}^* + \boldsymbol{\beta}_2^T \mathbf{u}_{i,2}^* , \tag{13}$$

where

$$k_\alpha = k_{11} + 2k_{12}\mu_\alpha + k_{22}\mu_\alpha^2,\ \boldsymbol{\beta}_1 = \begin{bmatrix} \beta_{11} \\ \beta_{21} \end{bmatrix},\ \boldsymbol{\beta}_2 = \begin{bmatrix} \beta_{12} \\ \beta_{22} \end{bmatrix},\ \mathbf{u}_i^* = \begin{bmatrix} U_{1i}^* \\ U_{2i}^* \end{bmatrix}. \tag{14}$$

Thus, substitution of Eq.(4a) into Eq.(13) leads to

$$f_i'' (z_\alpha) = \frac{1}{\pi} Im \left\{ \boldsymbol{\beta}_A^T < \frac{1}{k_\alpha (z_\alpha - \hat{z}_\alpha)} > \mathbf{A}^T \right\} \mathbf{i}_i, \tag{15}$$

where

$$\boldsymbol{\beta}_A^T = \boldsymbol{\beta}_1^T \mathbf{A} + \boldsymbol{\beta}_2^T \mathbf{A} < \mu_\alpha > . \tag{16}$$

In Eq.(15), Im{ } denotes the operation of taking imaginary part of the complex variable in the curly bracket; $\mathbf{i}_i$ is the unit base vector for the unit load applied in the x_i direction. As a result, direct integrations of Eq. (16) yield

$$f_i(z_\alpha) = \frac{1}{\pi} Im \left\{ \boldsymbol{\beta}_A^T < k_\alpha^{-1} (z_\alpha - \hat{z}_\alpha)[\ln(z_\alpha - \hat{z}_\alpha) - 1] > \mathbf{A}^T \right\} \mathbf{i}_i. \tag{17}$$

Performing spatial differentiations upon f results in

$$f_{i,1}(z_\alpha) = \frac{1}{\pi} Im \left\{ \boldsymbol{\beta}_A^T < k_\alpha^{-1} \ln(z_\alpha - \hat{z}_\alpha) > \mathbf{A}^T \right\} \mathbf{i}_i \tag{18a}$$

$$f_{i,2}(z_\alpha) = \frac{1}{\pi} Im \left\{ \boldsymbol{\beta}_A^T < \mu_\alpha k_\alpha^{-1} \ln(z_\alpha - \hat{z}_\alpha) > \mathbf{A}^T \right\} \mathbf{i}_i. \tag{18b}$$

Up to this point, there is still one more issue regarding the validity of the transformation that needs to be resolved As pointed out by Shiah and Tan (1999), the discontinuity along the branch cut of the logarithmic function in the domain will invalidate the use of the Green's Theorem to make such a transformation. In other words, the condition for the identity to hold true lies in the analyticity of the integrand throughout the whole domain. As has been discussed by Shiah and Tan

(1999), this issue can be resolved by simply re-defining the branch cut such that it is directed in the outward normal direction. However, such a treatment does not provide the general resolution especially when the boundary surface is concave or multiply connected in geometry. Consider the general case when the negative x-axis ($x = x_1 - \hat{x}_1$) cuts through the domain so that the intersected region is bounded by $[a_1, b_1], \ldots [a_m, b_m]$. As a consequence, taking the similar treatment as Shiah and Tan (1999) yields a series of extra line integrals added to the transformed BIE, expressed as

$$\begin{aligned} &c_{ij}u_j + \int_\Gamma T^*_{ij}u_j d\Gamma \\ &= \int_\Gamma U^*_{ij}t_j \, d\Gamma + \int_\Gamma \left(\Theta k_{jk} f_{i,k} n_j - f_i k_{jk} \Theta_{,j} n_k\right) d\Gamma + \sum_{n=1}^{m} \int_{a_n}^{b_n} L_i(x)\, dx, \end{aligned} \tag{19}$$

where

$$L_i(x) = -q_i k_{jk} \Theta_{,j} n_k + \Theta k_{jk} q_{i,k} n_j, \tag{20a}$$

$$\begin{aligned} &q_i = -2xRe\left\{\boldsymbol{\beta}_A^T < k_\alpha^{-1} > \mathbf{A}^T\right\} \mathbf{i}_i, \\ &q_{i,1} = -2Re\left\{\boldsymbol{\beta}_A^T < k_\alpha^{-1} > \mathbf{A}^T\right\} \mathbf{i}_i,\ q_{i,2} = -2Re\left\{\boldsymbol{\beta}_A^T < \mu_\alpha k_\alpha^{-1} > \mathbf{A}^T\right\} \mathbf{i}_i. \end{aligned} \tag{20b}$$

To this end, Eq.(19) is a truly boundary integral equation that can be solved for boundary unknowns via the usual BEM analysis. Next, a few numerical examples are provided for illustrating the validity of the derived formulations.

3 Numerical examples

For verifying the veracity of the transformed BIE, a few tests were carried out, where all material properties as tabulated in Table 1 just followed those used by Shiah and Tan (1999) The illustrations are separated into two parts. The former targets demonstration of the mathematical validity of the derived formulations, whereas the latter is for showing our successful implementation For these purposes, two example cases were studied as described in what follows.

Table 1: Material properties for the numerical examples

E_{11} (GPa)	E_{22} (GPa)	ν_{12}	G_{22} (GPa)	α_{11}	α_{22}	k_{11}	k_{12}
55	21	0.25	9.7	6.3×10^{-6} (/°C)	20×10^{-6} (/°C)	3.46 (W/m°C)	0.35 (W/m°C)

3.1 Case 1

For the first example (Fig.1) consider a (2m×2m) square plate under the plane stress condition. For treating general anisotropy, the principal axes are assumed to be rotated by 20 counterclockwise. For the choice of defining the coordinate origin at its center, the temperature is assumed to be distributed by

$$\Theta = 3x_1^2 - 5.7223x_1x_2 - 5x_2^2, \tag{21}$$

which satisfies Eq.(2) in accordance with the conductivities defined in the global Cartesian coordinates. Also shown in Fig.1 is the boundary discretization for the BEM modeling, where only 8 quadratic isoparametric elements are used. For showing the veracity of the volume-to-surface integral transformation, computations of the both, namely the volume integral as well as the transformed boundary ones, were carried out for all16 source points. As mentioned earlier for treating the discontinuity issue, the boundary integrals with the addition of the extra line integral were evaluated. Table 2 lists the results computed for all source points. As can be seen in Tab.2, the numerical values computed by both methods agree very minor discrepancy.

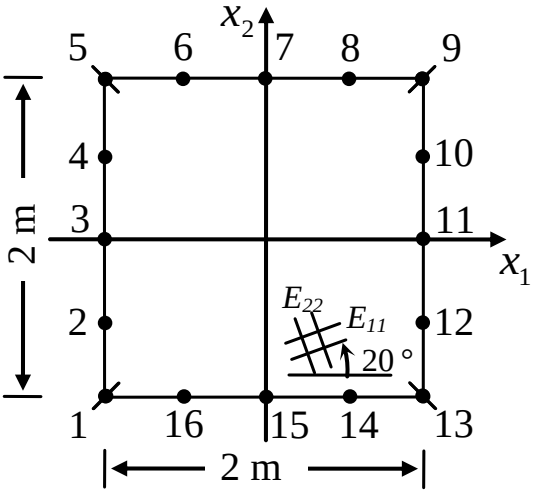

Figure 1: BEM mesh for computing the boundary integrals

For further illustration of our implementation to analyze a more general case, consider the heat conduction problem, depicted in Fig.2, with the boundary conditions: Θ=100˚C and 0˚C are specified on AB and CD, respectively, while the other surfaces are insulated.

For the elastic boundary conditions, all surfaces excluding the surface AB, assumed to be free of tractions, are constrained in their normal directions. Also shown in Fig.2 is the boundary discretization, where only 28 quadratic elements are employed. The principal axes are arbitrarily rotated by 60 counterclockwise to yield

$$\beta_{11} = 4.6375 \times 10^5 \text{ Pa}, \quad \beta_{12} = \beta_{21} = -6.9867 \times 10^2 \text{ Pa}, \quad \beta_{22} = 4.6294 \times 10^5 \text{ Pa}. \tag{22}$$

Table 2: Numerical values of the volume integral and the boundary integrals - Case1

Node	Coord.	V_1			V_2		
		Eq.(7)	Eq.(12)	% Diff.	Eq.(7)	Eq.(12)	% Diff.
1	(-1.0,-1.0)	5.707E-06	5.694E-06	0.23%	5.888E-06	5.884E-06	0.06%
2	(-1.0,-0.5)	8.300E-06	8.298E-06	0.02%	-1.427E-05	-1.427E-05	0.00%
3	(-1.0, 0.0)	2.700E-06	2.707E-06	0.26%	-1.088E-05	-1.088E-05	0.03%
4	(-1.0, 0.5)	-9.607E-07	-9.553E-07	0.56%	-1.285E-06	-1.282E-06	0.18%
5	(-1.0, 1.0)	-5.442E-07	-5.418E-07	0.45%	4.752E-06	4.754E-06	0.04%
6	(-0.5, 1.0)	6.556E-06	6.557E-06	0.01%	-5.193E-06	-5.193E-06	0.00%
7	(0.0, 1.0)	7.398E-06	7.403E-06	0.07%	-1.536E-05	-1.536E-05	0.00%
8	(0.5, 1.0)	3.478E-06	3.482E-06	0.10%	-1.754E-05	-1.754E-05	0.00%
9	(1.0, 1.0)	-5.707E-06	-5.694E-06	0.23%	-5.888E-06	-5.884E-06	0.06%
10	(1.0, 0.5)	-8.300E-06	-8.298E-06	0.02%	1.427E-05	1.427E-05	0.00%
11	(1.0, 0.0)	-2.700E-06	-2.707E-06	0.26%	1.088E-05	1.088E-05	0.03%
12	(1.0,-0.5)	9.607E-07	9.553E-07	0.56%	1.285E-06	1.282E-06	0.18%
13	(1.0,-1.0)	5.442E-07	5.418E-07	0.45%	-4.752E-06	-4.754E-06	0.04%
14	(0.5, -1.0)	-6.556E-06	-6.557E-06	0.01%	5.193E-06	5.193E-06	0.00%
15	(0.0, -1.0)	-7.398E-06	-7.403E-06	0.07%	1.536E-05	1.536E-05	0.00%
16	(-0.5, -1.0)	-3.478E-06	-3.482E-06	0.10%	1.754E-05	1.754E-05	0.00%

To verify the BEM results, the problem was also analyzed using ANSYS, commercial software based on the finite element method. For the ANSYS analysis, a total number of 10^4 PLANE223 elements were employed. For the comparison, the total displacements, $U_0 = \sqrt{u_1^2 + u_2^2}$, calculated for all sides are plotted in Fig.3.

Displayed in Fig. 4(a) and Fig. 4(b) are the resulting stresses calculated for $\overline{\text{AB}} - \overline{\text{DC}}$ and $\overline{\text{BC}} - \overline{\text{AD}}$, respectively. As can be seen from these plots, analyses

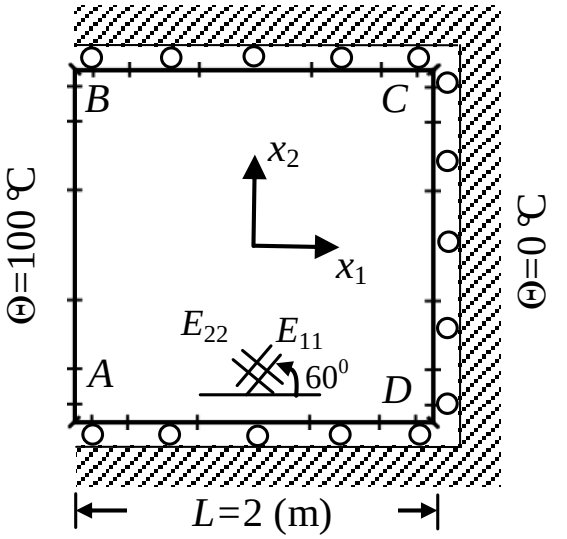

Figure 2: Problem definition and the BEM mesh for Case 1

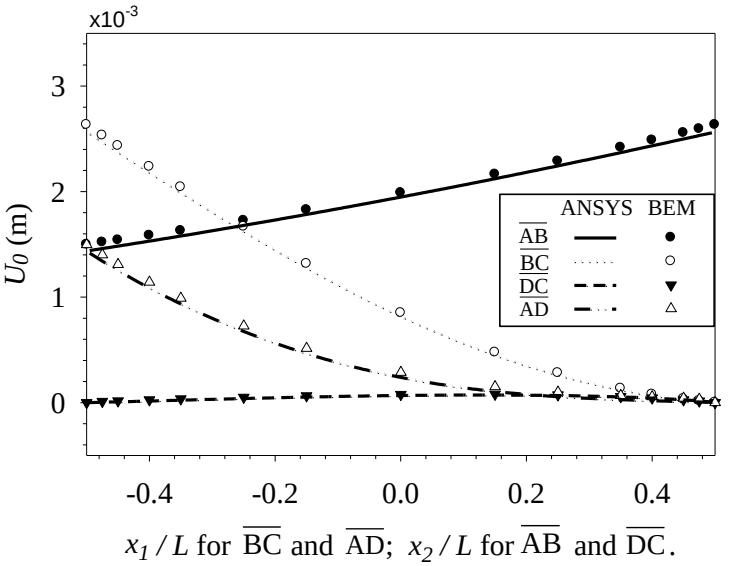

Figure 3: Displacements on the boundary- Case 1

by the both approaches are in excellent agreements, which have indeed confirmed the validity of our BEM analysis. The only obvious discrepancies in the calculated stresses occur at places near corners, where discontinuities are present; otherwise, all the BEM-calculated stresses at other places are very satisfactory indeed. For yielding more accurate results, more refined meshes, of course, are necessary especially near the corners. Since this issue is beyond the scope of this paper, the details will not be further discussed. Next, another example case will be analyzed to show the capability of the present approach in treating a multiply connected domain.

3.2 Case 2

For further demonstration of our implementation to analyze a more complicated geometry, the second case treats a concentric hollow disk as schematically shown in Fig. 5(a). For the boundary conditions, the outer surface is fully constrained and the inner is assumed to be free of tractions. Suppose the temperature changes of 100°C and 0°C are prescribed over the outside and the inside surface, respectively. Also, the principal axes are rotated by 30^0 counterclockwise to yield

$$\beta_{11} = 4.6294 \times 10^5 \text{ Pa}, \quad \beta_{12} = \beta_{21} = -6.9867 \times 10^2 \text{ Pa}, \quad \beta_{22} = 4.6375 \times 10^5 \text{ Pa}. \tag{23}$$

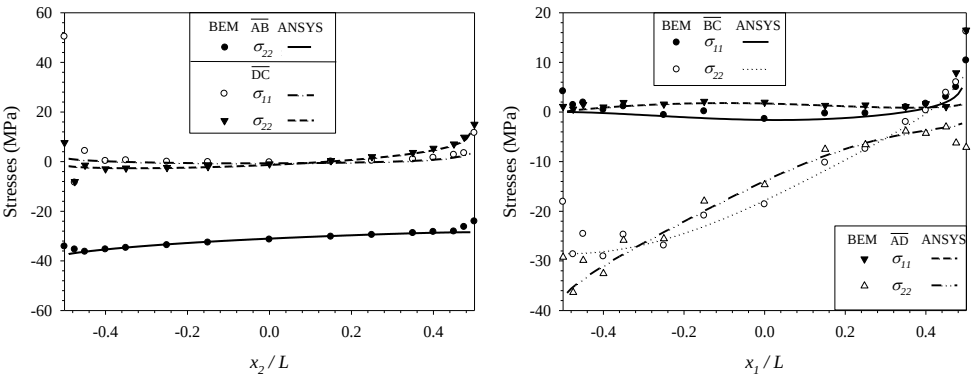

(a) (b)

Figure 4: Stress distributions on edges- Case 1: (a) for $\overline{AB} - \overline{DC}$, (b) for $\overline{BC} - \overline{AD}$.

As shown in Fig. 5, only 32 quadratic elements were used for the BEM modeling. Again, for providing comparison of results by an independent approach, the problem was also analyzed using ANSYS, where 7294 PLANE223 elements were used.

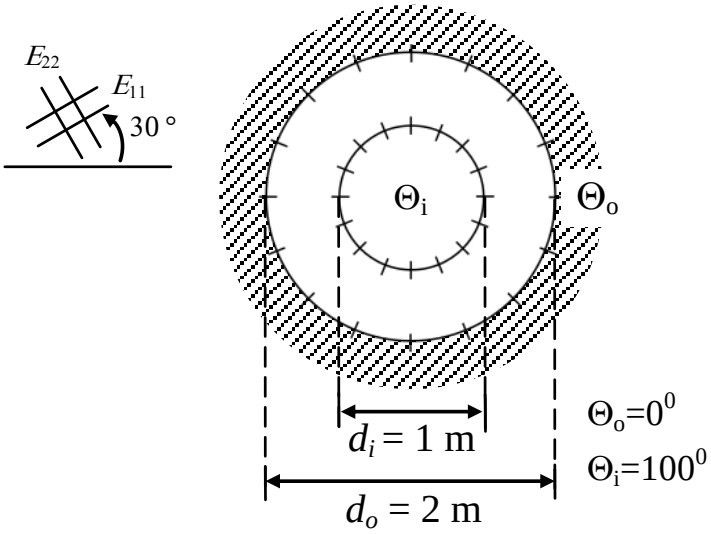

Figure 5: Problem definition and the BEM mesh for Case 2.

Figure 6 displays the calculated displacements on the inner surface as a function of θ, being the angle measured counterclockwise from the x_1-axis.

The corresponding hoop stresses on the inner surface calculated by the BEM and ANSYS are plotted altogether in Fig. 7(a) for comparison. Also, all the stresses computed for the constrained outside surface are displayed in Fig. 7(b).

As expected, the results obtained by both approaches are in good agreement. As aforementioned for Case 1, more refined BEM meshes can always be employed to increase accuracy of analysis; the present analysis by the coarse meshes is simply to show our successful implementation and the veracity of formulations.

4 Conclusive remarks

For the 2D thermoelastic BEM analysis, it is well known that the thermal effect reveals itself as a domain integral. To restore the BEM's feature of boundary discretization, the domain integral needs to be transformed to the boundary. In this paper, a direct analytical transformation for 2D anisotropic thermoelasticity involving no coordinate transformation is presented. All kernel functions, including the newly constructed one, are based on the Stroh formalism. Since no coordinate transformation is involved, the present approach appears to be more straightforward especially when the thermal field is directly calculated without resorting to the tech-

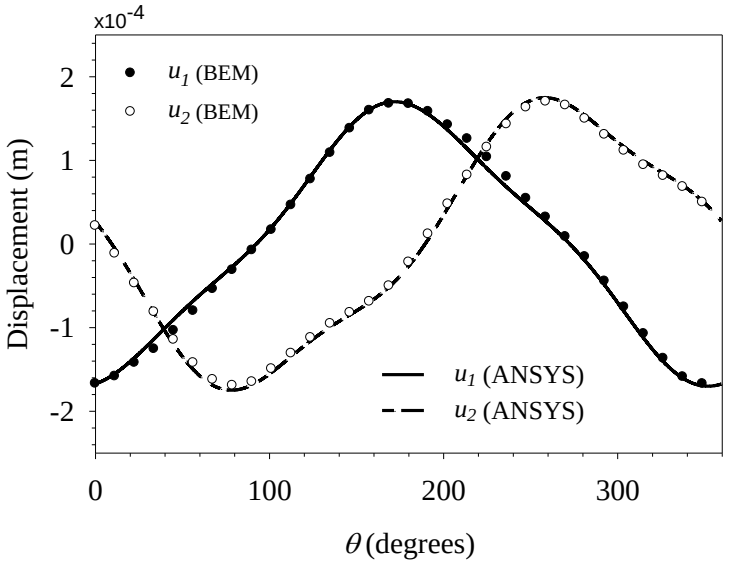

Figure 6: Displacements on the inner surface-Case 2.

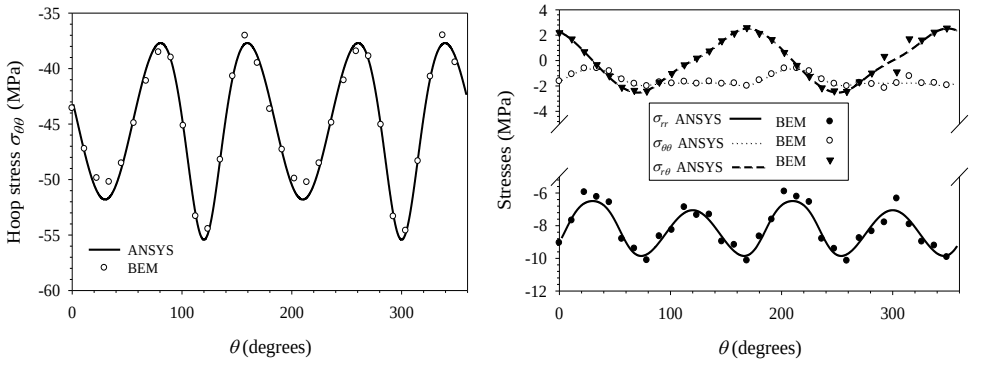

Figure 7: Distributions of stresses on the surfaces- Case 2, (a) hoop stress on the inner surface; (b) stresses on the outside surface.

nique of domain mapping. The derived formulations have been implemented in the BEM. The successful implementation is demonstrated by a few examples, showing that the BEM analyses are indeed in satisfactory agreements with the ANSYS analysis.

Acknowledgement: The authors gratefully acknowledge the financial supports from the Ministry of Science and Technology (NSC 102-2221-E-006-290-MY3 and No. 101-2221-E-006-056-MY3).

References:

Deb, A.; Banerjee, P. K. (1990): BEM for general anisotropic 2Delasticity using particular integrals. *Commun. Appl. Num. Meth.*, vol. 6, pp.111-119.

Gipson, G. S.; Camp, C. V.(1985): Effective use of Monte Carlo Quadrature for body force integrals occurring in integralform of elastostatics. *Proc. 7th Int. Conf. On Boundary Elements*, pp.17-26.

Hwu, C. (2010): *Anisotropic Elastic Plates*, Springer, NewYork.

Lachat, J. C. (1975): *Further development of the boundary integral technique for elastostatics*. Ph.D. Thesis, Southampton University.

Lekhnitskii, S. G. (1981): *Theory of elasticity of an anisotropic body*, Mir Publishers, Moscow.

Nowak, A. J.; Brebbia, C. A. (1989): The multiple-reciprocity method-a new approach for transforming BEM domain integrals to the boundary. *Eng. Anal. Bound. Elem.*, vol.6, pp.164-167.

Rizzo, F. J.; Shippy, D. J. (1977) An advanced boundary integral equation method for three-dimensional thermoelasticity. *Int. J. Numerical Methods Engng.*, vol. 11, pp. 1753-1768.

Shiah, Y. C.; Tan, C. L. (1999): Exact boundary integral transformation of the thermoelasticdomain integral in BEM for general 2D anisotropic elasticity. *Computational Mechanics*, vol. 23, pp.87-96.

Shiah, Y. C.; Guao, T. L.; Tan, C. L (2005): Two-dimensional BEM thermoelastic analysis of anisotropic media with concentrated heat sources. *CMES: Computer Modeling in Engineering & Sciences*, vol. 7, no. 3, pp. 321-338.

Shiah, Y. C.; Tan, C. L. (2000): Fracture mechanics analysis in 2-D anisotropic thermoelasticity using BEM. *CMES: Computer Modeling in Engineering & Sciences*, vol.1, no.3, pp.91-99.

Shiah, Y. C.; Tan, C. L.; Lee, R. F. (2010): Internal point solutions for displacements and stresses in 3D anisotropic elastic solids using the boundary element

method. *CMES: Computer Modeling in Engineering & Sciences*, vol. 69, no. 2, pp. 167-198.

Shiah, Y. C.; Tan, C. L. (2012): Boundary element method for thermoelastic analysis of three-dimensional transversely isotropic solids. *International Journal of Solids and Structures*, vol. 49, pp. 2924-2933.

Zhang, J. J.; Tan, C. L.; Afagh, F. F. (1997): Treatment of body-force volume integrals in BEM by exact transformation for 2D anisotropic elasticity. *Int. J. Numerical Methods Engng*., vol. 40, pp. 89-109.